Physical Science International Journal

25(1): 23-38, 2021; Article no.PSIJ.65917
ISSN: 2348-0130

Strain Field Development of a Rectangular Dislocation Loop in a Semi-Infinite Medium with Verification

Luo Li[1] and Tariq A. Khraishi[1*]

[1]Mechanical Engineering Department, University of New Mexico, Albuquerque, New Mexico, USA.

Authors' contributions

This work was carried out in collaboration between both authors. Author LL was responsible for the derivations, verifications and initial paper write-up. Author TAK designed this research and contributed to paper writing and editing. Both authors read and approved the final manuscript.

Article Information

DOI: 10.9734/PSIJ/2021/v25i130234
Editor(s):
(1) Dr. Pratima Parashar Pandey, Dr. APJ Abdul Kalam Technical University, India.
(2) Dr. Thomas F. George, University of Missouri, USA.
Reviewers:
(1) Altaf Ahmad Bhat, Islamic University of Science and Technology (IUST), India.
(2) Bushra Eesa, University of Technology, Iraq.
(3) Ezinna Lucky Efurumibe, Michael Okpara University of Agriculture, Nigeria.
Complete Peer review History: http://www.sdiarticle4.com/review-history/65917

Original Research Article

Received 20 December 2020
Accepted 23 February 2021
Published 03 April 2021

ABSTRACT

This paper considers a rectangular Volterra dislocation loop lying beneath and parallel to a free surface in a semi-infinite material. The paper utilizes the displacement field of an infinitesimal dislocation loop to obtain the strain field and then integrate over a finite rectangular area. For the loop, it can have three non-zero Burgers vector components. The stress field is also obtained from Hooke's law for isotropic materials. Analytical and numerical verifications of the strain and stress fields are performed. In addition, the effect of the free surface on stresses is displayed versus depth from the surface. Verification includes satisfaction of the zero-traction boundary condition, the stress equilibrium equations and the strain compatibility equations.

Keywords: Rectangular dislocation loop; half medium; strain/stress field; numerical/analytical verification.

**Corresponding author: E-mail: khraishi@unm.edu;*

1. INTRODUCTION

Dislocation loops are defects in the material, associating the collapse of a large number of point defects into lower energy defect structures. A rectangular dislocation loop is a closed loop composed of four straight dislocation lines. Dislocation lines have to end on free surfaces, grain boundaries, or form a closed loop inside a material. They cannot end inside the crystal [1]. In this work, the development of the strain field of a Volterra-type rectangular dislocation loop parallel to the free surface of half medium, and having three non-zero Burgers vector components, is focused on.

Several dislocation problems in terms of material type, geometry and size have been developed for decades. In the early years, research on infinite isotropic materials was studied by different researchers. Development of the elastic fields of infinite screw and edge dislocations in an infinite isotropic medium were provided [2-4]. Furthermore, integral equations for finding the displacement field (the Burgers equation) and the stress field (the Peach-Koehler equation) of a closed dislocation loop (of any shape) in an *infinite* isotropic material have been provided by Hirth JP et al. [2].

A couple of researchers have studied different kinds of dislocation loop problems applying various techniques. Initially [5-6], researched the prismatic circular loop. The circular glide loop was initially investigated by Keller JM [7] Kröner E [8], which was later corrected in [9-10]. Khraishi TA et al. [11] Khraishi TA et al. [12] corrected some earlier work in a more recent study of the displacement and stress fields of glide and prismatic circular dislocation loops. The displacement field of a rectangular dislocation loop of the Volterra type in an infinite medium was obtained by Khraishi TA et al. [13], which contains a solid angle term. The above references in this paragraph all focused on an infinite material.

One application for dislocation loops is its use in the "collocation point" method that is used to resolve traction-free surface problems in a semi-infinite material simulated with the 3-D DDD method via a surface mesh of rectangular/triangular dislocation loops [14-18]. Siddique AB et al. [19] extended the collocation-point method to deal with curved free surfaces. For circular dislocation loops, they were used for modeling pile-ups around rigid cylindrical particles [20] and for modeling Frank sessile loops which are caused by irradiation damage in some metals [21-23].

As for studies involving dislocations near a free surface, Yoffe EH et al. [24] developed the elastic fields of a dislocation terminating on a free surface (for any Burgers vector). Groves PP et al. [25] studied the effects of free surfaces on a dislocation loop. Maurissen Y et al. [26] Maurissen Y et al. [27] obtained the correction terms of the stress field of a dislocation half-line and segment parallel and perpendicular to a free surface in a semi-infinite elastic medium. Comninou M et al. [28] presented the formulations for the elastic fields of an angular dislocation in an isotropic half-space. Gosling TJ et al. [29] determined the stresses due to an arbitrary dislocation in a semi-infinite medium as a line integral along the dislocation. Jing et al. [30] found the displacement field of a rectangular dislocation loop parallel to a free surface.

In this paper, the strain components of a rectangular dislocation loop parallel to a free surface are obtained. Also, analytical and numerical verifications for the strain field are performed. The verification is to ensure that the Strain Compatibility Equations are satisfied. Then, the stress field, obtained via Hooke's law using the strain developed herein, is verified using the Equilibrium Equations and the zero-traction condition on the free surface. Moreover, plots reflecting the effect of the free surface correction term are presented at different depths beneath the surface.

2. METHODOLOGY

- **Development of the strains of the sub-surface rectangular dislocation loop**

The dislocation problem under consideration is shown in Fig. 1. The figure shows a rectangular dislocation loop (also described as a "finite-sized dislocation loop") in a semi-infinite isotropic medium and which is below the free surface. This Volterra-type dislocation loop has three Burgers vector components b_x, b_y and b_z . Also, it has a dimension 2*a* in the *x*-direction and a dimension 2*b* in the *y*-direction. The line sense of the dislocation loop is shown by the arrow around the dislocation loop. The goal of this problem is to obtain the strain components at an arbitrary material field point P. Note that in this paper, x_1 and *x* are used interchangeably, so are x_2 and *y*, and so are x_3 and z. Analogously for x'_1 and x', and so on.

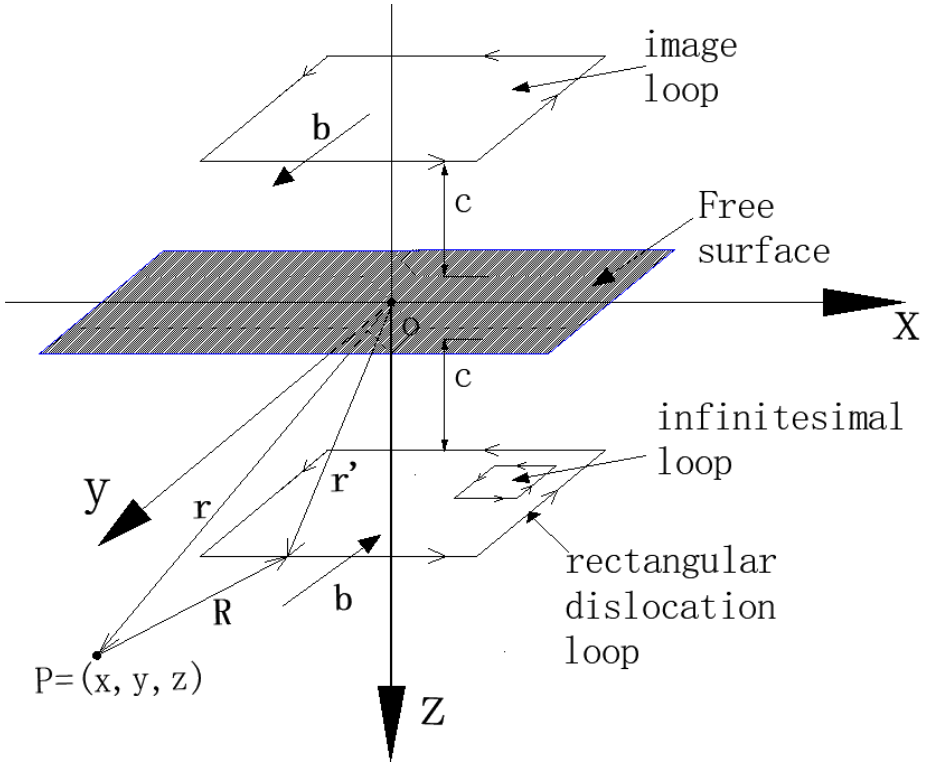

Fig. 1. A rectangular dislocation loop with an arbitrary Burgers vector, below a free surface. Also, an image dislocation loop with opposite Burgers vector is shown above the surface. An infinitesimal dislocation loop used in the integration is also shown

To find the total strain field due to the subsurface rectangular dislocation loop, one can sum up the three contributions of the total strain field as in the following:

$$\boldsymbol{\epsilon} = \boldsymbol{\epsilon}^{inf} + \boldsymbol{\epsilon}^{imag} + \boldsymbol{\epsilon}^{s} \quad (1)$$

Where the superscript 'inf' refers to the strain solution of a rectangular dislocation loop in an infinite medium, not in a half medium as shown in Fig. 1. The superscript 'imag' refers to the strain solution of an image dislocation loop with an opposite Burgers vector laying above the surface. And the 's' superscript refers to surface correction term which ensures the zero-traction condition on the free surface, i.e. the image loop by itself does not annul all the stress traction components on the surface.

Let's focus on the correction term in the above equation first. Bacon and Grove provided an equation for the displacement surface correction term of a subsurface infinitesimal dislocation loop with area dS [25]:

$$du_i^s = -kx_3^{'}(1-2\delta_{j3})[A_{i3}\left(\frac{1}{R}\right)_{,ij} - \left(\frac{x_3}{R}\right)_{,ij3}] \quad (2)$$

where, $k = b_j\, dS/4\pi(1-\nu)$, $A_{ij} = 2\nu + 4(1-\nu)\delta_{ij}$, $dS = dx_1^{'}dx_2^{'}$, $R^2 = (x_1 - x_1^{'})^2 + (x_2 - x_2^{'})^2 + (x_3 + x_3^{'})^2$. δ_{ij} is the ij^{th} component of the Kronecker delta.

Equation (2) can be written explicitly as follows:

When
i=1:
j=1:

$$du_1^s = -\frac{x_3^{'}\, b_x\, dS}{4\pi(1-\nu)}\left[2\nu\left(\frac{1}{R}\right)_{,11} - \left(\frac{x_3}{R}\right)_{,113}\right] \quad (3)$$

i=1:
j=2:

$$du_1^s = -\frac{x_3^{'}\, b_y\, dS}{4\pi(1-\nu)}\left[2\nu\left(\frac{1}{R}\right)_{,12} - \left(\frac{x_3}{R}\right)_{,123}\right] \quad (4)$$

i=1:
j=3:

$$du_1^s = \frac{x_3' b_z dS}{4\pi(1-\nu)}\left[2\nu\left(\frac{1}{R}\right)_{,13} - \left(\frac{x_3}{R}\right)_{,133}\right] \quad (5)$$

When

i=2:
j=1:

$$du_2^s = -\frac{x_3' b_x dS}{4\pi(1-\nu)}\left[2\nu\left(\frac{1}{R}\right)_{,21} - \left(\frac{x_3}{R}\right)_{,213}\right] \quad (6)$$

i=2:
j=2:

$$du_2^s = -\frac{x_3' b_y dS}{4\pi(1-\nu)}\left[2\nu\left(\frac{1}{R}\right)_{,22} - \left(\frac{x_3}{R}\right)_{,223}\right] \quad (7)$$

i=2:
j=3:

$$du_2^s = \frac{x_3' b_z dS}{4\pi(1-\nu)}\left[2\nu\left(\frac{1}{R}\right)_{,23} - \left(\frac{x_3}{R}\right)_{,233}\right] \quad (8)$$

When

i=3:
j=1:

$$du_3^s = -\frac{x_3' b_x dS}{4\pi(1-\nu)}\left[\left(2\nu + 4(1-\nu)\right)\left(\frac{1}{R}\right)_{,31} - x3R,313\right] \quad (9)$$

i=3:
j=2:

$$du_3^s = -\frac{x_3' b_y dS}{4\pi(1-\nu)}\left[\left(2\nu + 4(1-\nu)\right)\left(\frac{1}{R}\right)_{,32} - x3R,323\right] \quad (10)$$

i=3:
j=3:

$$du_3^s = \frac{x_3' b_z dS}{4\pi(1-\nu)}\left[\left(2\nu + 4(1-\nu)\right)\left(\frac{1}{R}\right)_{,33} - x3R,333\right] \quad (11)$$

To find the strain field for the correction term of an infinitesimal loop, the tensorial small strain definition is applied:

$$d\epsilon_{ij}{}^s = \frac{1}{2}\left(\frac{\partial du_i^s}{\partial x_j} + \frac{\partial du_j^s}{\partial x_i}\right) \quad (12)$$

As for the strain surface *correction* term in equation (1) for the finite rectangular loop, it can be obtained with integration via:

$$\boldsymbol{\epsilon} = \int_A d\boldsymbol{\epsilon}^{\boldsymbol{s}} \quad (13)$$

Where *A* is the area of integration. For the infinite term in equation (1), the elastic fields of a rectangular dislocation loop have been obtained in [31]. Hence, the development of the infinite term in equation (1) is not repeated here for brevity. If one has the solution for the *infinite* term in equation (1), one can easily obtain the *image* term which has an opposite Burgers vector and opposite 'z' value to infinite term. If one has the expressions for the three terms contributing to equation (1), then the *total* strain field can be easily determined from the sum of these terms.

3. RESULTS AND DISCUSSION

Based on the above, the strain field of a rectangular dislocation loop has been obtained with integrations and other manipulations all performed using the strong symbolic engine of the mathematical software Mathematica. Such results are provided in the Appendix. If one is interested in the stress field (which is not shown herein explicitly like the strains for brevity sake), one can use Hooke's law for isotropic materials:

$$\sigma_{ij} = \lambda\epsilon_{kk}\delta_{ij} + 2\mu\epsilon_{ij} \quad (14)$$

where $\lambda = \frac{E\nu}{(1+\nu)(1-2\nu)}$, $\mu = \frac{E}{2(1+\nu)}$ Here, δ_{ij} is the *ij*th component of the Kronecker delta, μ is shear modulus, ϵ_{kk} is the dilatation or the volumetric strain, and E is Young's modulus.

3.1 Strain Compatibility Equations Verification

The equations of compatibility can be written in indicial notation as [32]:

$$\epsilon_{ij,kl} - \epsilon_{jl,ik} - \epsilon_{ik,jl} + \epsilon_{kl,ij} = 0 \quad (15)$$

This equation can be expanded over the repeated indices and written explicitly as six different/unique equations:

$$\frac{\partial^2\epsilon_{xx}}{\partial y^2} + \frac{\partial^2\epsilon_{yy}}{\partial x^2} = 2\frac{\partial^2\epsilon_{xy}}{\partial x\partial y} \quad (16)$$

$$\frac{\partial^2\epsilon_{xx}}{\partial z^2} + \frac{\partial^2\epsilon_{zz}}{\partial x^2} = 2\frac{\partial^2\epsilon_{xz}}{\partial x\partial z} \quad (17)$$

$$\frac{\partial^2\epsilon_{zz}}{\partial y^2} + \frac{\partial^2\epsilon_{yy}}{\partial z^2} = 2\frac{\partial^2\epsilon_{zy}}{\partial z\partial y} \quad (18)$$

$$\frac{\partial^2\epsilon_{xx}}{\partial y\partial z} + \frac{\partial^2\epsilon_{yz}}{\partial x^2} = \frac{\partial^2\epsilon_{xz}}{\partial x\partial y} + \frac{\partial^2\epsilon_{xy}}{\partial x\partial z} \quad (19)$$

$$\frac{\partial^2 \epsilon_{yy}}{\partial x \partial z} + \frac{\partial^2 \epsilon_{xz}}{\partial y^2} = \frac{\partial^2 \epsilon_{xy}}{\partial y \partial z} + \frac{\partial^2 \epsilon_{yz}}{\partial x \partial y} \quad (20)$$

$$\frac{\partial^2 \epsilon_{zz}}{\partial x \partial y} + \frac{\partial^2 \epsilon_{xy}}{\partial z^2} = \frac{\partial^2 \epsilon_{xz}}{\partial y \partial z} + \frac{\partial^2 \epsilon_{yz}}{\partial x \partial z} \quad (21)$$

These equations should be satisfied at every material point in the solid. To verify the developed strain solution, one can see if equations (16-21) are identically zero using either analytical or numerical methods. For the analytical method, the equations are so humongous that Mathematica is not able to reduce them to 0. However, for any given line in space along the *x*-, *y*- or *z*-directions, Mathematica identically converts the compatibility equations to zero. Hence analytical verification of the compatibility equations is feasible.

Alternatively, numerical verifications can also be shown by plotting equations (16-21) along any plane in the material to see if the equations give a zero result. Fig. 2 shows such plotting for $b_z \neq 0$. The figure shows that the compatibility equations are satisfied. Note that given the combination of Burgers vector components and compatibility equations a total of eighteen plots are minimally generated. Therefore, only three plots for one of the Burgers vector components are shown here for brevity.

3.2 Equilibrium Equations Verification

To verify the strain field developed in this paper, one can use equation (14) to obtain the stress field and see if the obtained stress field can satisfy the equilibrium equations. The partial differential equations of static equilibrium in a solid material can be written in indicial notation as:

$$\sigma_{ij,j} = \frac{\partial \sigma_{ij}}{\partial x_j} = 0 \quad (22)$$

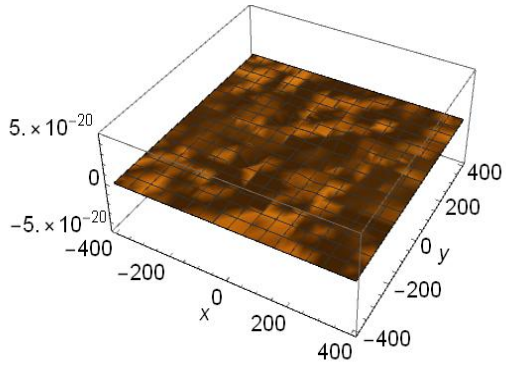

Fig. 2.1. Plot of equation (16)

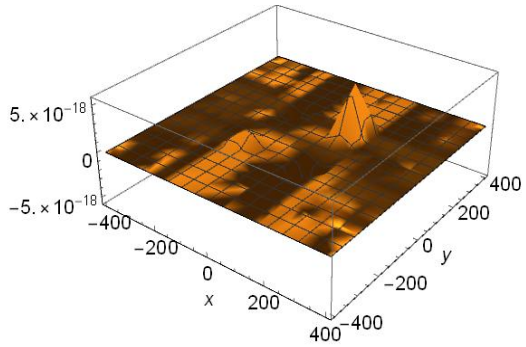

Fig. 2.2. Plot of equation (19)

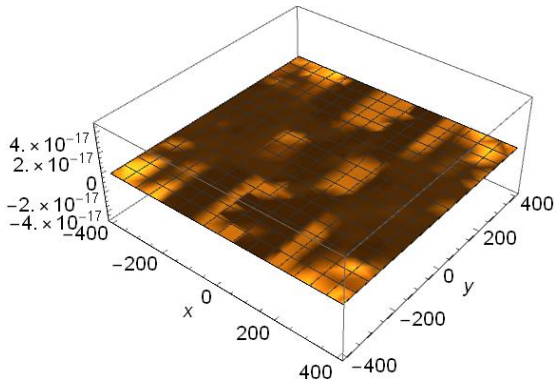

Fig. 2.3. Plot of equation (20)

For these plots, the following values were chosen: $a = b = 100b_z$, $z' = c = 10b_z$, $b_x = b_y = 0$, $b_z = 1$, $\nu = 0.3$, $\mu = G = 100$, $z = 11b_z$, $-4a \leq x \leq 4a$, $-4b \leq y \leq 4b$

If the last equation is expanded on the repeated indices then the resulting three equations are:

$$\frac{\partial \sigma_{xx}}{\partial x} + \frac{\partial \sigma_{xy}}{\partial y} + \frac{\partial \sigma_{xz}}{\partial z} = 0 \tag{23}$$

$$\frac{\partial \sigma_{yx}}{\partial x} + \frac{\partial \sigma_{yy}}{\partial y} + \frac{\partial \sigma_{yz}}{\partial z} = 0 \tag{24}$$

$$\frac{\partial \sigma_{zx}}{\partial x} + \frac{\partial \sigma_{zy}}{\partial y} + \frac{\partial \sigma_{zz}}{\partial z} = 0 \tag{25}$$

This is keeping in mind the symmetry of the stress tensor, i.e. $\sigma_{ij} = \sigma_{ji}$. These equations should be satisfied at every material point of a solid in equilibrium. To verify the stress solution given by equation (14), one can see if equations (23-25) are identically satisfied either using analytical or numerical methods. For the analytical method, the equations are all reduced to zero by utilizing Mathematica. Analogously, if one considers any line in space, the three equilibrium equations also equate analytically to zero. Hence, analytical verification of the equilibrium equations is feasible.

Alternatively, numerical verification can also be made by plotting equations (23-25) along any plane in the material to see if the equations show a zero result. Fig. 3 shows such plotting for $b_y \neq 0$. The figure shows that the equilibrium equations are satisfied. Note that given the combination of Burgers vector components and equilibrium equations a total of nine plots are minimally generated. Therefore, only three plots for one of the Burgers vector components are shown here for brevity.

3.3 Free-Traction Condition on the Free Surface

Another way to verify the strain field developed herein is to plug the obtained strain field solution into equation (14) to get the stress solution and check if the stress solution satisfies the free-traction condition on the free surface. The stress traction $\vec{T}$ at the free surface can be written as:

$$\vec{T} = \boldsymbol{\sigma}\vec{n} \tag{26}$$

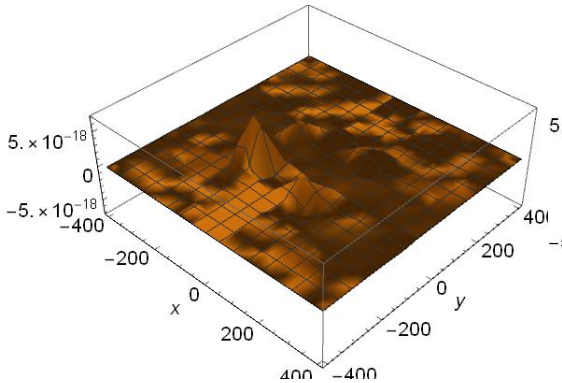

Fig. 3.1. Plot of equation (23)

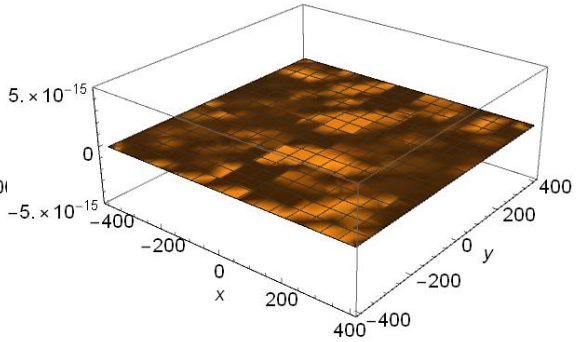

Fig. 3.2. Plot of equation (24)

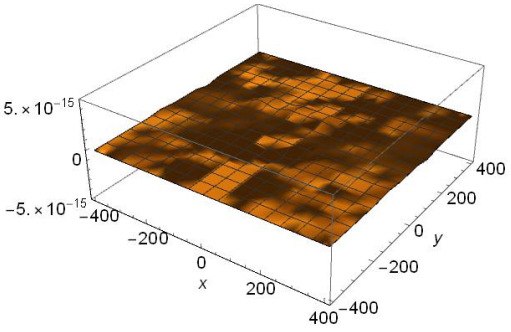

Fig. 3.3. Plot of equation (25)

For these plots, the following values were chosen: $a = b = 100b_y$, $z' = c = 10b_y$, $b_x = b_z = 0$, $b_y = 1$, $\nu = 0.3$, $\mu = 100$, $z = 11b_y$, $-4a \leq x \leq 4a$, $-4b \leq y \leq 4b$

Which should be $\vec{0}$ at the free surface. Here, $\boldsymbol{\sigma}$ is given by equation (14). The unit normal vector at the free surface is {0 0 -1}, see Fig. 1. In this case, σ_{xz} σ_{yz} and σ_{zz} components should all be zero at the free surface. To make sure that these three stress components are zero on the surface, one could use equation (14) and specify z = 0 in it and see if it reduces to 0 for each of the three stress components. Unfortunately, since the final solutions of stress field obtained by equation (14) are too long, Mathematica was not able to analytically simplify these stress components at z = 0 down to 0 value even if one waited more than 24 hours for the simplification result. Alternatively, if one considers arbitrary lines along the x and y directions on the free surface, these stress components did reduce to zero identically. In addition to the analytical verification, surface plots of the three stress field components on the free surface were generated. This is a numerical verification as all such three stress values should be zero. The plots in Fig. 4 are done for $b_x \neq 0$.

3.4 Nomralized Plots for the Stress Field of a Subsurface Rectangular Dislocation Loop

Note that by taking the developed total strain solution (the three parts of it) and substituting them into equation (14), one can then separate the stresses into three parts and write an equation similar to equation (1):

$$\boldsymbol{\sigma} = \boldsymbol{\sigma}^{inf} + \boldsymbol{\sigma}^{imag} + \boldsymbol{\sigma}^{s} \tag{27}$$

As equation (27) shows, total stress field for the subsurface rectangular dislocation loop involves three terms which are the infinite term, the image term and the surface correction term.

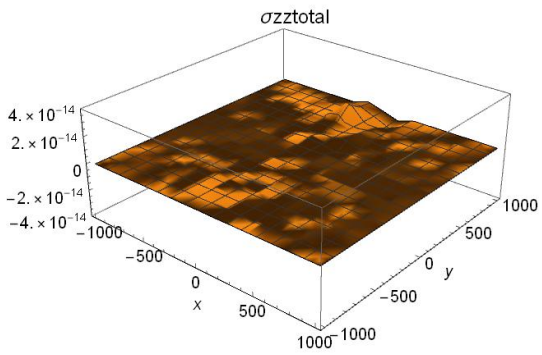

Fig. 4.1. Plot of the equation for σ_{zz}

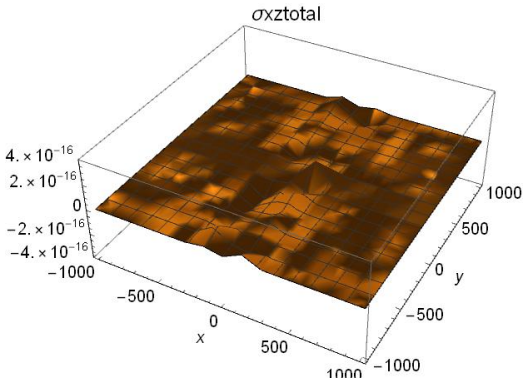

Fig. 4.2. Plot of the equation for σ_{xz}

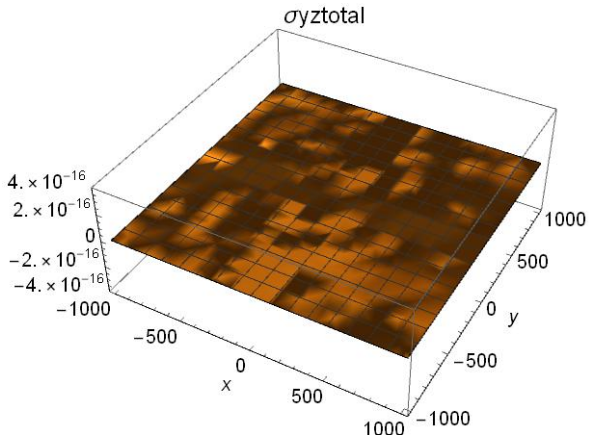

Fig. 4.3. Plot of the equation for σ_{yz}

For these plots, the following values were chosen: $a = b = 100b_x$, $z' = c = 10b_x$, $b_y = b_z = 0$, $b_x = 1$, $\nu = 0.3$, $\mu = 100$, $z = 0$, $-10a \leq x \leq 10a$, $-10b \leq y \leq 10b$

To investigate the stress field of a rectangular dislocation loop in an isotropic half medium at different z depths, one can plot separately the total stress and its parts along the *x* and *y* directions. Fig. 5 shows the effect of depth on the different stresses (total stress, infinite term, image term and stress correction term). Fig. 6 shows the effect of depth on the stress correction term. For the plots in Figs. 5 and 6, the following values were chosen: $a = b = 100b_x$, $z' = c = 400b_x$, $b_y = b_z = 0$, $b_x = 1$, $\nu = 0.3$, $\mu = 1$, $-10a \le x \le 10a$, $y = 0$.

For the plots in Fig. 7, the following values were chosen: $a = b = 100b_z$, $z' = c = 400b_z$, $b_y = b_x = 0$, $b_z = 1$, $\nu = 0.3$, $\mu = 1$, $-10b \le y \le 10b$, $x = 0$. Similar to Figs. 5 and 6, these figures also show the effect of depth on the stress correction term but for $b_z \neq 0$.

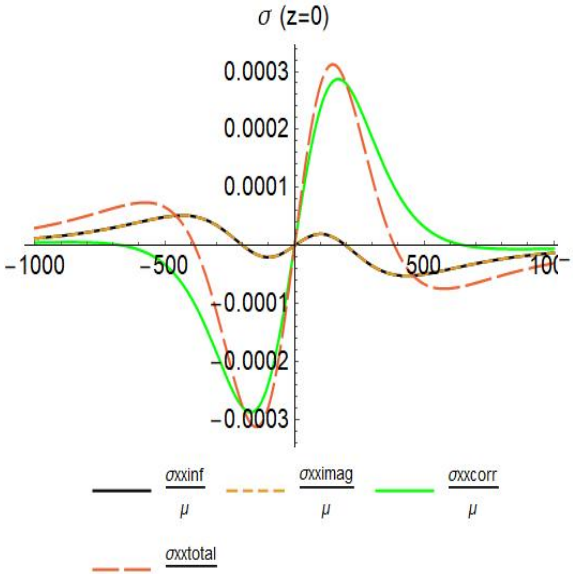

Fig. 5.1. σ_{xx} for z/c=0

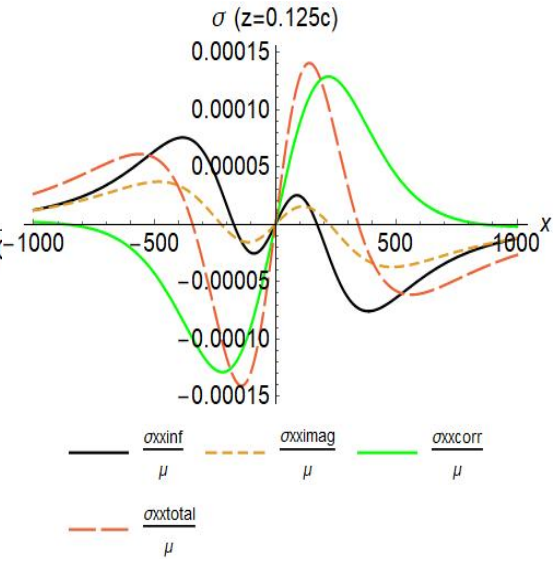

Fig. 5.2. σ_{xx} for z/c=0.125

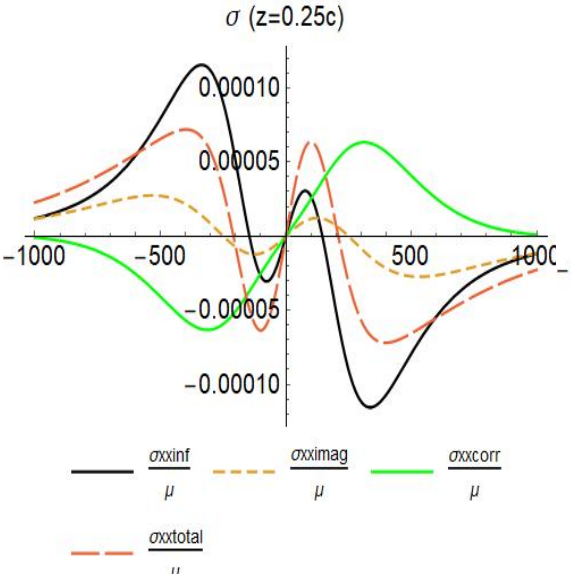

Fig. 5.3. σ_{xx} with z/c=0.25

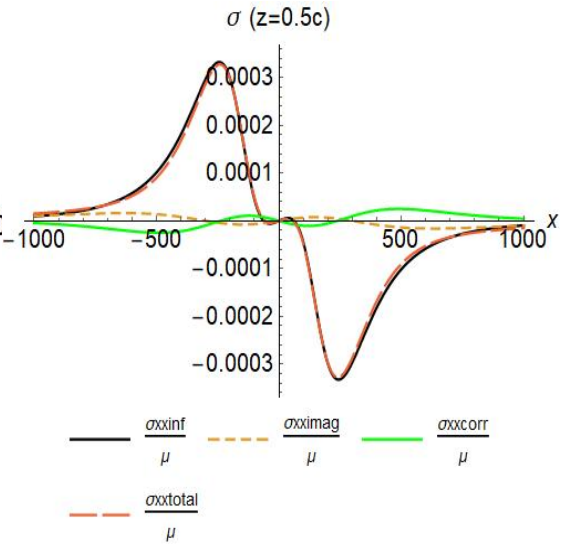

Fig. 5.4. σ_{xx} for z/c=0.5

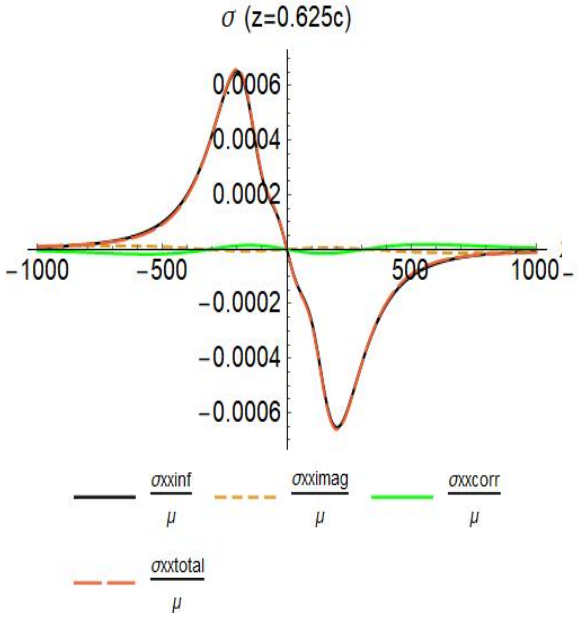

Fig. 5.5. σ_{xx} for z/c=0.625

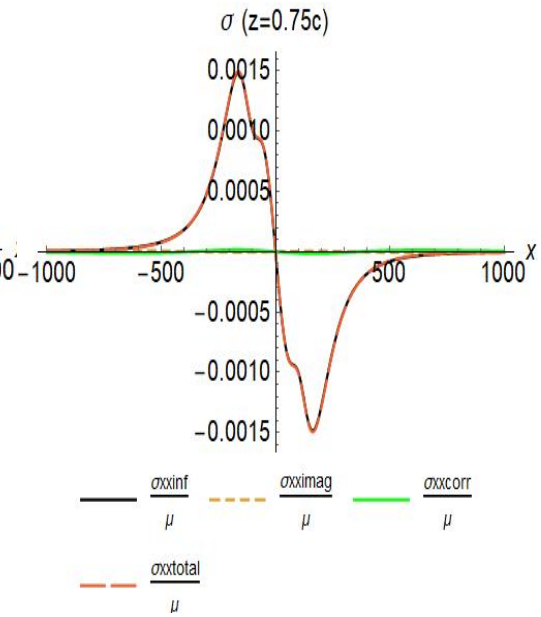

Fig. 5.6. σ_{xx} for z/c=0.75

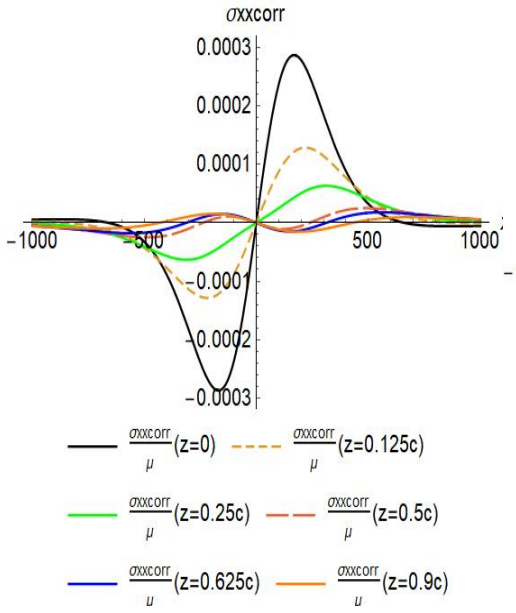

Fig. 6.1. σ_{xx} surface correction (varying z), $b_x \neq 0$

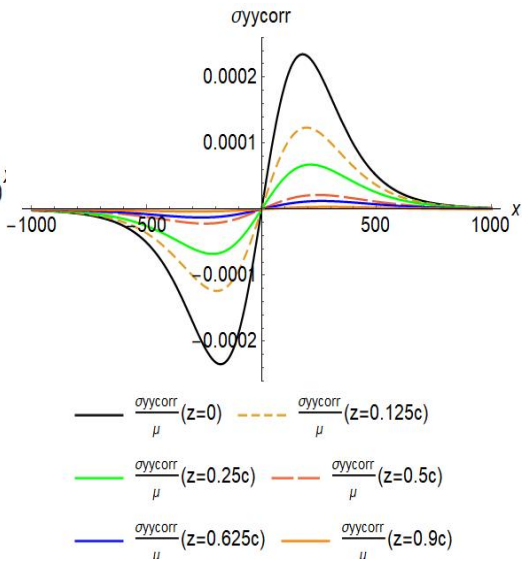

Fig. 6.2. σ_{yy} surface correction (varying z), $b_x \neq 0$

As the plots in Fig. 5 show, the correction term nearly dominates the total stress value of a dislocation loop at the surface, while the effect of the infinite term is much lesser. However, as the material point in question gets further away from the free surface, the infinite term gradually dominates the total stress value while the effect of the surface correction term on the total stress gets weaker. Indeed, at high depths closer to the dislocation loop in the half medium, the total stress value is almost all due to the infinite term. Fig. 6, which focuses on the stress correction term only, shows a similar trend for this term as it is usually highest on the surface and diminishes close the dislocation loop. Note that some stress components are not drawn here since they are identically equal to zero along a line parallel to *x* with *y*=0 and $b_x \neq 0$. Fig. 7 is similar to Figs. 5 and

6 but is done along a line parallel to the y-axis with x=0 and $b_z \neq 0$. This figure also shows that the stress correction term diminishes fast from the free surface. In Fig. 7, the stress correction terms for σ_{xy} and σ_{xz} are identically zero along a line parallel to the y-axis with x=0 and $b_z \neq 0$ and hence are not plotted here. Moreover, the plots of stress components for b_y are not shown here for brevity since the plots are similar to the ones of stress components for b_x.

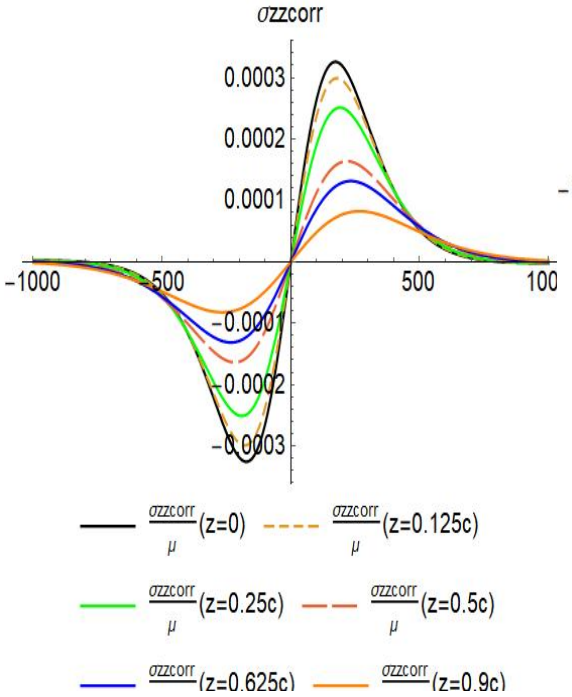

Fig. 6.3. σ_{zz} surface correction (varying z), $b_x \neq 0$

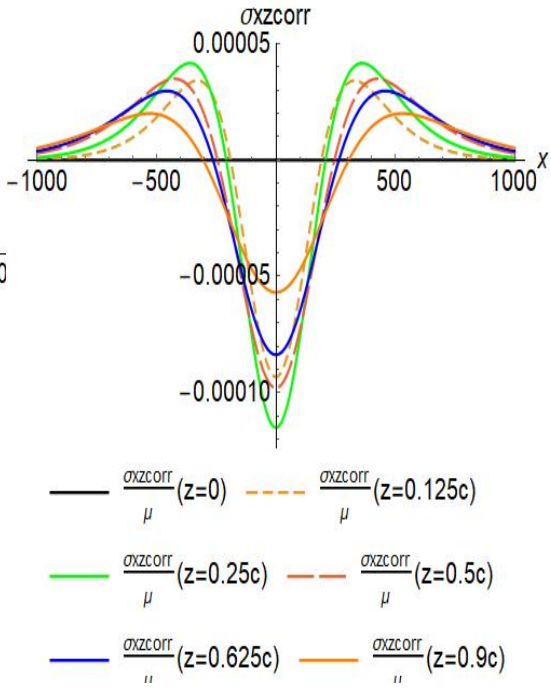

Fig. 6.4. σ_{xz} surface correction (varying z), $b_x \neq 0$

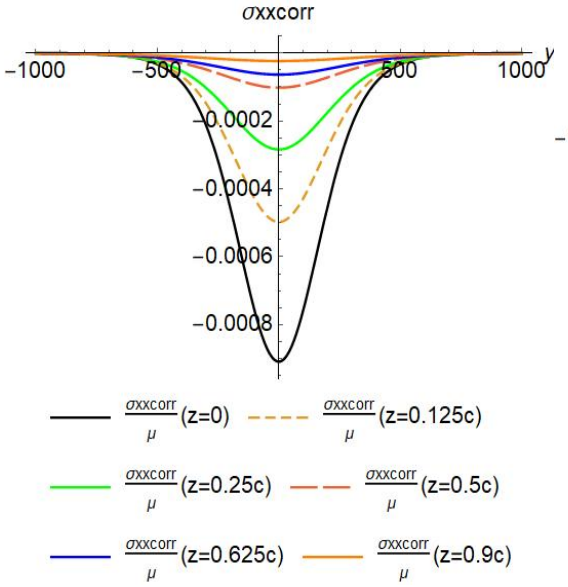

Fig. 7.1. σ_{xx} surface correction (varying z), $b_z \neq 0$

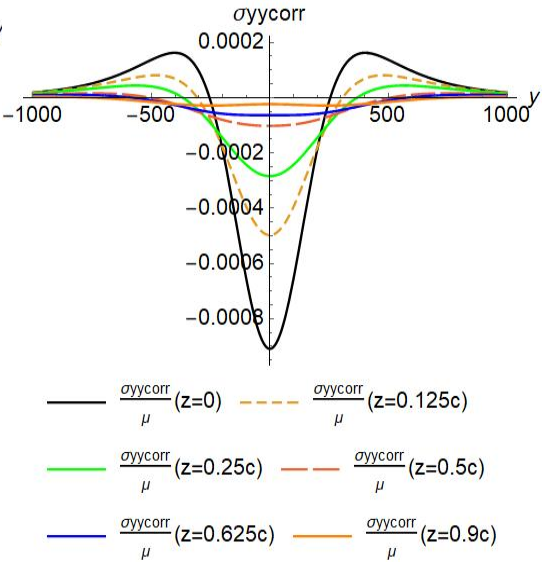

Fig. 7.2. σ_{yy} surface correction (varying z), $b_z \neq 0$

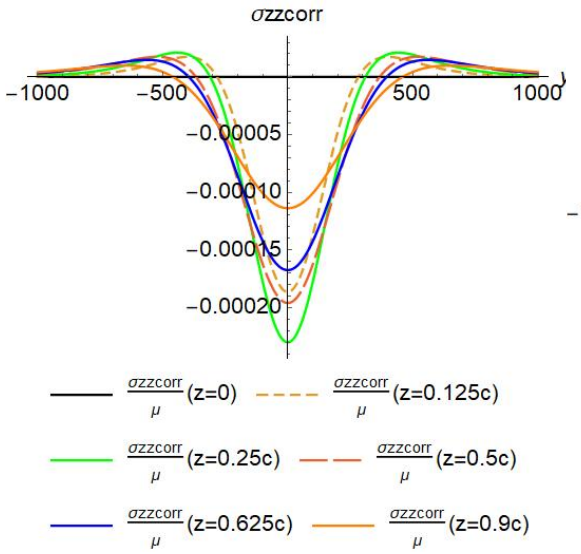

Fig. 7.3. σ_{zz} surface correction (varying z), $b_z \neq 0$

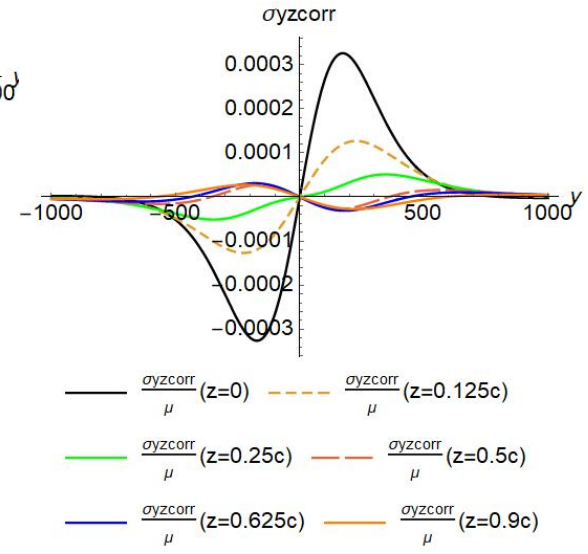

Fig. 7.4. σ_{yz} surface correction (varying z), $b_z \neq 0$

4. CONCLUSIONS

In conclusion, the strain field of a subsurface rectangular dislocation loop parallel to the free surface in a half medium has been obtained in this paper. The developed strain field is verified using different fundamental equations of continuum mechanics. Firstly, the strain solution is verified using the Strain Compatibility Equations, which are the equations relating the different strain components' spatial distribution. As the results show, the strain solution developed herein satisfies the Compatibility Equations. Secondly, one can also verify the strain field by plugging the strain solution into Hooke's Law to obtain the stress field. Then, one can check if this stress field satisfies the Equilibrium Equations and the zero-traction condition on the free surface. As the results show, the stress field obtained in this manner does indeed satisfy the Equilibrium Equations and the free-traction condition. The last conclusion from this work regards the decay rate of the surface effects on the total stress. The surface effects diminish quickly away from the surface as one gets closer and closer to the subsurface dislocation loop.

COMPETING INTERESTS

Authors have declared that no competing interests exist.

REFERENCES

1. Meyers MA, Chawla KK. Mechanical Behavior of Materials. 2nd edition. University of Cambridge, UK; 2009.
2. Hirth JP, Lothe J. Theory of dislocations. 5th edition. Krieger Publishing Company, Malabar, Florida; 1982.
3. Hull D, Bacon DJ. Introduction to Dislocations. University of Liverpool, UK; 2011.
4. Weertman J, Weertman JR. Elementary Dislocation Theory. Oxford University Press, Oxford; 1992.
5. Kroupa F. Circular edge dislocation loop. Czech J Phys B. 1960;10:284–293.
6. Bullough R, Newman RC. The spacing of prismatic dislocation loops. Phil Mag. 1960;5(57):921–926.
7. Keller JM. Unpublished; 1957.
8. Kröner E. Kontinuumstheorie Der Versetzungen Und Eigenspannungen. Springer-Verlag, Berlin; 1958.
9. Kroupa F. Interaction between prismatic dislocation loops and straight dislocations 1 Phil Mag. 1962;7(77):783–801.
10. Marcinkowski MJ, Sree Harsha KS. Properties of finite circular dislocation glide loops. J Appl Phys. 1968;39(3):1775–1783.
11. Khraishi TA, Hirth JP, Zbib HM, Khaleel MA. The displacement, and strain-stress fields of a general circular Volterra dislocation loop. International Journal of Engineering Science. 2000;38(3):251–266.

12. Khraishi TA, Zbib HM, Hirth JP, De La Rubia TD. The stress field of a general circular Volterra dislocation loop: Analytical and numerical approaches. Phil Mag Lett. 2000;80(2):95–105.
13. Khraishi TA, Zbib HM. The displacement field of a rectangular Volterra dislocation loop. Phil Mag Lett. 2002;82(5):265–277.
14. Khraishi TA, Zbib HM, De La Rubia TD. The treatment of traction-free boundary condition in three-dimensional dislocation dynamics using generalized image stress analysis. Materials Science and Engineering A. 2001;309-310:283-87.
15. Khraishi TA, Zbib HM. Free surface effects in 3d dislocation dynamics: Formulation and Modeling. Journal of Engineering Materials and Technology (JEMT). 2002; 124(3):342-51.
16. Yan L, Khraishi TA, Shen Y-L, Horstemeyer MF. A distributed-dislocation method for treating free-surface image stresses in 3D dislocation dynamics simulations. Modelling and Simulation in Materials Science and Engineering. 2004; 12(4):289-301.
17. Siddique AB, Khraishi T. Numerical methodology for treating static and dynamic dislocation problems near a free surface. Journal of Physics Communications. 2020;4(5):055005. DOI:10.1088/2399-6528/ab8ff9.
18. Siddique AB, Khraishi T. A mesh-independent brute-force approach for traction-free corrections in dislocation problems. Modeling and Numerical Simulation of Material Science. 2021;11(1): 1-18. DOI: 10.4236/mnsms.2021.111001.
19. Siddique AB, Khraishi T. Screw dislocations around voids of any shape: A Generalized Numerical approach. Forces in Mechanics. 2021;3:100014. DOI:https://doi.org/10.1016/j.finmec.2021.100014.
20. Khraishi TA, Zbib HM. Dislocation dynamics simulations of the interaction between a short rigid fiber and a glide circular dislocation pile-up. Computational Materials Science. 2002; 24(3):310-22.
21. De La Rubia TD, Zbib HM, Khraishi TA, Wirth BD, Victoria M, Caturla MJ. Multiscale Modelling of Plastic Flow Localization in Irradiated Materials. Nature. 2000;406(6798):871-74.
22. Khraishi TA, Zbib HM, De La Rubia TD, Victoria M. Modeling of irradiation-induced hardening in metals using dislocation dynamics. Philosophical Magazine Letters. 2001;81(9):583-93.
23. Khraishi TA, Zbib HM, De La Rubia TD, Victoria M. Localized deformation and hardening in irradiated metals: Three-dimensional discrete dislocation dynamics simulations. Metallurgical and Materials Transactions B. 2002;33(2):285-96.
24. Yoffe, EH. A dislocation at a free surface. The Philosophical Magazine. 1961;69(6): 1147–55.
25. Groves PP, Bacon DJ. The dislocation loop near a free surface. Philosophical Magazine. 1970;22(175):83–91.
26. Maurissen Y, Capella L. Stress field of a dislocation segment parallel to a free surface. Philosophical Magazine. 1974; 29(5):1227–29.
27. Maurissen Y, Capella L. Stress field of a dislocation segment perpendicular to a free surface. Philosophical Magazine. 1974; 30(3):679–83.
28. Comninou M, Dundurs J. The angular dislocation in a half space. J. Elasticity. 1975;5:203–16.
29. Gosling TJ, Willis JR. A line-integral representation for the stresses due to an arbitrary dislocation in an isotropic half-space. J. Mech. Phys. Solids. 1994;42(8): 1199-1221.
30. Jing P, Khraishi TA. The elastic fields of sub-surface dislocation loops: A comparison between analytical continuum-theory solutions and atomistic calculations. Int. J. Theoretical and Applied Multiscale Mechaics. 2009;1(1):71-85.
31. Li L, Khraishi TA. The stress field of a rectangular dislocation loop in an infinite medium: analytical solution with verification. Journal of Materials Science Research and Reviews. 2021;7(1):47-59. Available:https://www.journaljmsrr.com/index.php/JMSRR/article/view/30172
32. Khraishi TA, Shen, YL. Introductory continuum mechanics with applications to elasticity. University Readers/Cognella, San Diego, California; 2011.

APPENDIX

Considering the Burgers vector component b_x:

$$\epsilon_{xx} = \frac{1}{4K1\pi} b_x c(-3\ p1\ \left(\frac{Q1^2}{A2^{5/2}B1} - \frac{Q2^2}{A4^{5/2}B2}\right) Q3\ z + 3p1\left(\frac{Q1^2}{A1^{5/2}B1} - \frac{Q2^2}{A3^{5/2}B2}\right) Q4\ z + \frac{Q3(Q1^4+p1(p1^2p2-6Q1^2z))}{\sqrt{A2}B1^3} - \frac{Q4(Q1^4+p1(p1^2p2-6Q1^2z))}{\sqrt{A1}B1^3} - \frac{Q3(Q2^4-p1(-p1^2p2+6Q2^2z))}{\sqrt{A4}B2^3} + \frac{Q4(Q2^4-p1(-p1^2p2+6Q2^2z))}{\sqrt{A3}B2^3} - \frac{Q3(-c^3z+cz(Q1^2-3z^2)-(Q1^2-z^2)^2-c^2(Q1^2+3z^2))}{A2^{3/2}B1^2} + \frac{Q4(-c^3z+cz(Q1^2-3z^2)-(Q1^2-z^2)^2-c^2(Q1^2+3z^2))}{A1^{3/2}B1^2} - \frac{Q3(c^3z-cz(Q2^2-3z^2)+(Q2^2-z^2)^2+c^2(Q2^2+3z^2))}{A4^{3/2}B2^2} + \frac{Q4(c^3z-cz(Q2^2-3z^2)+(Q2^2-z^2)^2+c^2(Q2^2+3z^2))}{A3^{3/2}B2^2}) + \frac{b_x cv}{2K1\pi}(\frac{Q1^2}{B1}(-\frac{Q3}{A2^{3/2}} + \frac{Q4}{A1^{3/2}}) + \frac{(-p1^2+Q1^2)}{B1^2}(-\frac{Q3}{\sqrt{A2}} + \frac{Q4}{\sqrt{A1}}) + \frac{Q2^2}{B2}(\frac{Q3}{A4^{3/2}} - \frac{Q4}{A3^{3/2}}) + \frac{(-p1^2+Q2^2)}{B2^2}(\frac{Q3}{\sqrt{A4}} - \frac{Q4}{\sqrt{A3}}));$$

$$\epsilon_{yy} = -\frac{b_x c\ K2}{4K1\pi}(-\frac{Q3}{A2^{3/2}} + \frac{Q3}{A4^{3/2}}) + \frac{b_x c\ K2}{4K1\pi}(-\frac{Q4}{A1^{3/2}} + \frac{Q4}{A3^{3/2}}) - \frac{3b_x c\ p1z}{4K1\pi}(-\frac{Q3}{A2^{5/2}} + \frac{Q3}{A4^{5/2}}) + \frac{3b_x c\ p1\ z}{4K1\pi}(-\frac{Q4}{A1^{5/2}} + \frac{Q4}{A3^{5/2}});$$

$$\epsilon_{zz} = \frac{b_x cK3\ p1^2Q3}{2A2^{3/2}B1K1\pi} - \frac{b_x cK3\ p1^2Q3}{2A4^{3/2}B2K1\pi} - \frac{b_x cK3(-p1^2+Q1^2)Q3}{2\sqrt{A2}B1^2K1\pi} + \frac{b_x cK3(-p1^2+Q2^2)Q3}{2\sqrt{A4}B2^2K1\pi} - \frac{b_x c\ p1(p1^2p3+p4Q2^2)Q3}{4A4^{3/2}B2^2K1\pi} - \frac{b_x cK3\ p1^2Q4}{2A1^{3/2}B1K1\pi} + \frac{b_x c\ K3p1^2Q4}{2A3^{3/2}B2K1\pi} + \frac{b_x cK3(-p1^2+Q1^2)Q4}{2\sqrt{A1}B1^2K1\pi} - \frac{b_x cK3(-p1^2+Q2^2)Q4}{2\sqrt{A3}B2^2K1\pi} + \frac{b_x c\ p1(p1^2p3+p4Q2^2)Q4}{4A3^{3/2}B2^2K1\pi} + \frac{b_x c\ p1Q3(p1^2p3+3Q1^2(c+2z))}{4A2^{3/2}B1^2K1\pi} - \frac{b_x c\ p1Q4(p1^2p3+3Q1^2(c+2z))}{4A1^{3/2}B1^2K1\pi} + \frac{b_x cQ3(-3Q1^4+p1(p1^2p5+6Q1^2z))}{4\sqrt{A2}B1^3K1\pi} - \frac{b_x cQ4(-3Q1^4+p1(p1^2p5+6Q1^2z))}{4\sqrt{A1}B1^3K1\pi} - \frac{b_x cQ3(-3Q2^4+p1(p1^2p5+6Q2^2z))}{4\sqrt{A4}B2^3K1\pi} + \frac{b_x cQ4(-3Q2^4+p1(p1^2p5+6Q2^2z))}{4\sqrt{A3}B2^3K1\pi} - \frac{3b_x c\ p1^3Q3z}{4(\pi-\pi\nu)}(-\frac{1}{A2^{5/2}B1} + \frac{1}{A4^{5/2}B2}) + \frac{3b_x c\ p1^3Q4z}{4(\pi-\pi\nu)}(-\frac{1}{A1^{5/2}B1} + \frac{1}{A3^{5/2}B2});$$

$$\epsilon_{xy} = \frac{b_x c}{4K1\pi}(-\frac{Q1}{A1^{3/2}} - \frac{Q2}{A3^{3/2}} + \frac{3p1Q1z}{A1^{5/2}} + \frac{3p1Q2z}{A3^{5/2}}) - \frac{b_x c}{4K1\pi}(-\frac{Q1}{A2^{3/2}} - \frac{Q2}{A4^{3/2}} + \frac{3p1Q1z}{A2^{5/2}} + \frac{3p1Q2z}{A4^{5/2}}) + \frac{b_x cv}{2K1\pi}(\frac{Q1}{A1^{3/2}} + \frac{Q2}{A3^{3/2}}) - \frac{b_x cv}{2K1\pi}(\frac{Q1}{A2^{3/2}} + \frac{Q2}{A4^{3/2}});$$

$$\epsilon_{xz} = \frac{b_x c\ p1Q1Q3(3A2-Q3^2)}{2A2^{3/2}B1^2K1\pi} + \frac{b_x c\ p1Q2Q3(3A4-Q3^2)}{2A4^{3/2}B2^2K1\pi} - \frac{b_x c\ p1Q1Q4(3A1-Q4^2)}{2A1^{3/2}B1^2K1\pi} - \frac{b_x c\ p1Q2Q4(3A3-Q4^2)}{2A3^{3/2}B2^2K1\pi} + \frac{3a\ b_x c\ p1^2Q3z}{4A4^{5/2}B1K1\pi} + \frac{3a\ b_x c\ p1^2Q3z}{4A4^{5/2}B2K1\pi} - \frac{3a\ b_x c\ p1^2Q4z}{4A1^{5/2}B1K1\pi} - \frac{3a\ b_x c\ p1^2Q4z}{4A3^{5/2}B2K1\pi} - \frac{3b_x c\ p1^2Q3xz}{4A2^{5/2}B1K1\pi} + \frac{3b_x c\ p1^2Q3xz}{4A4^{5/2}B2K1\pi} + \frac{3b_x c\ p1^2Q4xz}{4A1^{5/2}B1K1\pi} - \frac{3b_x c\ p1^2Q4xz}{4A3^{5/2}B2K1\pi} - \frac{a\ b_x c\ Q3(3A2-Q3^2)(p6(c^2+Q1^2)-z^3)}{4A2^{3/2}B1^3K1\pi} + \frac{a\ b_x c\ Q4(3A1-Q4^2)(p6(c^2+Q1^2)-z^3)}{4A1^{3/2}B1^3K1\pi} + \frac{b_x c\ Q3(3A2-Q3^2)x(p6(c^2+Q1^2)-z^3)}{4A2^{3/2}B1^3K1\pi} - \frac{b_x c\ Q4(3A1-Q4^2)x(p6(c^2+Q1^2)-z^3)}{4A1^{3/2}B1^3K1\pi} - \frac{a\ b_x c\ Q3(3A4-Q3^2)(p6(c^2+Q2^2)-z^3)}{4A4^{3/2}B2^3K1\pi} + \frac{a\ b_x c\ Q4(3A3-Q4^2)(p6(c^2+Q2^2)-z^3)}{4A3^{3/2}B2^3K1\pi} - \frac{b_x c\ Q3(3A4-Q3^2)x(p6(c^2+Q2^2)-z^3)}{4A4^{3/2}B2^3K1\pi} + \frac{b_x c\ Q4(3A3-Q4^2)x(p6(c^2+Q2^2)-z^3)}{4A3^{3/2}B2^3K1\pi};$$

$$\epsilon_{yz} = \frac{3b_x c\ p1}{2K1\pi}(\frac{1}{3A3^{3/2}} - \frac{1}{3(A3-4ax)^{3/2}}) - \frac{3b_x c\ p1}{2K1\pi}(\frac{1}{3A4^{3/2}} - \frac{1}{3(A4-4ax)^{3/2}}) + \frac{b_x c}{4K1\pi}(\frac{p6}{A1^{3/2}} + \frac{-2c-3z}{A3^{3/2}} - \frac{3p1^2z}{A1^{5/2}} + \frac{3p1^2z}{A3^{5/2}}) - \frac{b_x c}{4K1\pi}(\frac{p6}{A2^{3/2}} + \frac{-2c-3z}{A4^{3/2}} - \frac{3p1^2z}{A2^{5/2}} + \frac{3p1^2z}{A4^{5/2}});$$

Considering the Burgers vector component b_y:

$$\epsilon_{xx} = \frac{3b_y c}{4K1\pi}(\frac{K2Q1}{3A1^{3/2}} + \frac{K2Q2}{3A3^{3/2}} + \frac{p1Q1z}{A1^{5/2}} + \frac{p1Q2z}{A3^{5/2}}) - \frac{3b_y c}{4K1\pi}(\frac{K2Q1}{3A2^{3/2}} + \frac{K2Q2}{3A4^{3/2}} + \frac{p1Q1z}{A2^{5/2}} + \frac{p1Q2z}{A4^{5/2}});$$

$$\epsilon_{yy} = -\frac{b_y cQ1(Q3^4-p1(-p1^2p2+6Q3^2z))}{4C1^3K1\pi\sqrt{C1+Q1^2}} - \frac{b_y cQ2(Q3^4-p1(-p1^2p2+6Q3^2z))}{4\sqrt{A4}C1^3K1\pi} + \frac{b_y cQ1(Q4^4+p1(p1^2p2-6Q4^2z))}{4C2^3K1\pi\sqrt{C2+Q1^2}} + \frac{b_y cQ2(Q4^4+p1(p1^2p2-6Q4^2z))}{4\sqrt{A3}C2^3K1\pi} - \frac{b_y cQ1(c^3z-cz(Q3^2-3z^2)+(Q3^2-z^2)^2+c^2(Q3^2+3z^2))}{4C1^2K1\pi(C1+Q1^2)^{3/2}} - \frac{b_y cQ2(c^3z-cz(Q3^2-3z^2)+(Q3^2-z^2)^2+c^2(Q3^2+3z^2))}{4A4^{3/2}C1^2K1\pi} - \frac{b_y cQ1(-c^3z+cz(Q4^2-3z^2)-(Q4^2-z^2)^2-c^2(Q4^2+3z^2))}{4C2^2K1\pi(C2+Q1^2)^{3/2}} - \frac{b_y cQ2(-c^3z+cz(Q4^2-3z^2)-(Q4^2-z^2)^2-c^2(Q4^2+3z^2))}{4A3^{3/2}C2^2K1\pi} + \frac{b_y cv}{2K1\pi}(\frac{Q1Q3^2}{A2^{3/2}C1} + \frac{Q2Q3^2}{A4^{3/2}C1} - \frac{Q1(p1^2-Q3^2)}{\sqrt{A2}C1^2} - \frac{Q2(p1^2-Q3^2)}{\sqrt{A4}C1^2} - \frac{Q1Q4^2}{A1^{3/2}C2} -$$

$$\frac{Q2Q4^2}{A3^{3/2}C2}+\frac{Q1(p1^2-Q4^2)}{\sqrt{A1}C2^2}+\frac{Q2(p1^2-Q4^2)}{\sqrt{A3}C2^2})-\frac{3b_yc\ p1Q2z}{4(\pi-\pi\nu)}(\frac{Q3^2}{A4^{5/2}C1}-\frac{Q4^2}{A3^{5/2}C2})-\frac{3b_yc\ p1Q1z}{4(\pi-\pi\nu)}(\frac{Q3^2}{C1(C1+Q1^2)^{5/2}}-\frac{Q4^2}{C2(C2+Q1^2)^{5/2}});$$

$$\epsilon_{zz}=$$
$$-\frac{b_ycK3p1^2Q1}{2C1K1\pi(C1+Q1^2)^{3/2}}+\frac{b_ycK3p1^2Q1}{2C2K1\pi(C2+Q1^2)^{3/2}}-\frac{b_ycK3p1^2Q2}{2A4^{3/2}C1K1\pi}+\frac{b_ycK3p1^2Q2}{2A3^{3/2}C2K1\pi}+\frac{b_ycK3Q1(-p1^2+Q3^2)}{2C1^2K1\pi\sqrt{C1+Q1^2}}+\frac{b_ycK3Q2(-p1^2+Q3^2)}{2\sqrt{A4}C1^2K1\pi}-$$
$$\frac{b_yc\ p1Q1(p1^2p3+p4Q3^2)}{4C1^2K1\pi(C1+Q1^2)^{3/2}}-\frac{b_yc\ p1Q2(p1^2p3+p4Q3^2)}{4A4^{3/2}C1^2K1\pi}-\frac{b_yc\ K3Q1(-p1^2+Q4^2)}{2C2^2K1\pi\sqrt{C2+Q1^2}}-\frac{b_yc\ K3Q2(-p1^2+Q4^2)}{2\sqrt{A3}C2^2K1\pi}+$$
$$\frac{b_yc\ p1Q1(p1^2p3+3Q4^2(c+2z))}{4C2^2K1\pi(C2+Q1^2)^{3/2}}+\frac{b_yc\ p1Q2(p1^2p3+3Q4^2(c+2z))}{4A3^{3/2}C2^2K1\pi}-\frac{b_yc\ Q1(-3Q3^4+p1(p1^2p5+6Q3^2z))}{4C1^3K1\pi\sqrt{C1+Q1^2}}-$$
$$\frac{b_yc\ Q2(-3Q3^4+p1(p1^2p5+6Q3^2z))}{4\sqrt{A4}C1^3K1\pi}+\frac{b_yc\ Q1(-3Q4^4+p1(p1^2p5+6Q4^2z))}{4C2^3K1\pi\sqrt{C2+Q1^2}}+\frac{b_yc\ Q2(-3Q4^4+p1(p1^2p5+6Q4^2z))}{4\sqrt{A3}C2^3K1\pi}-$$
$$\frac{3b_yc\ p1^3Q1z}{4(\pi-\pi\nu)}(\frac{1}{C1(C1+Q1^2)^{5/2}}-\frac{1}{C2(C2+Q1^2)^{5/2}})-\frac{3b_yc\ p1^3Q2z}{4(\pi-\pi\nu)}(\frac{1}{A4^{5/2}C1}-\frac{1}{A3^{5/2}C2});$$

$$\epsilon_{xy}=$$
$$-\frac{b_yc\ Q3(Q1^2+Q3^2-p1(-c+2z))}{4A2^{5/2}K1\pi}+\frac{b_yc\ Q3(Q2^2+Q3^2-p1(-c+2z))}{4A4^{5/2}K1\pi}+\frac{b_yc\ Q4(Q1^2+Q4^2-p1(-c+2z))}{4A1^{5/2}K1\pi}-$$
$$\frac{b_yc\ Q4(Q2^2+Q4^2-p1(-c+2z))}{4A3^{5/2}K1\pi}-\frac{b_yc\ \nu}{2K1\pi}(-\frac{Q3}{A2^{3/2}}+\frac{Q3}{A4^{3/2}})+\frac{b_yc\ \nu}{2K1\pi}(-\frac{Q4}{A1^{3/2}}+\frac{Q4}{A3^{3/2}});$$

$$\epsilon_{xz}=\frac{b_yc\ p1}{2K1\pi}(-\frac{1}{A1^{3/2}}+\frac{1}{A3^{3/2}})-\frac{b_yc\ p1}{2K1\pi}(-\frac{1}{A2^{3/2}}+\frac{1}{A4^{3/2}})+\frac{b_yc}{4K1\pi}(\frac{p6}{A1^{3/2}}+\frac{p7}{A3^{3/2}}-\frac{3p1^2z}{A1^{5/2}}+\frac{3p1^2z}{A3^{5/2}})-\frac{b_yc}{4K1\pi}(\frac{p6}{A2^{3/2}}+\frac{p7}{A4^{3/2}}-\frac{3p1^2z}{A2^{5/2}}+\frac{3p1^2z}{A4^{5/2}});$$

$$\epsilon_{yz}=$$
$$\frac{b\ b_yc\ p1Q1(3p1^2+2Q1^2+3Q3^2)}{2C1^2K1\pi(C1+Q1^2)^{3/2}}+\frac{b\ b_yc\ p1Q2(3p1^2+2Q2^2+3Q3^2)}{2A4^{3/2}C1^2K1\pi}+\frac{b\ b_yc\ p1Q1(3p1^2+2Q1^2+3Q4^2)}{2C2^2K1\pi(C2+Q1^2)^{3/2}}+$$
$$\frac{b\ b_yc\ p1Q2(3p1^2+2Q2^2+3Q4^2)}{2A3^{3/2}C2^2K1\pi}+\frac{b_yc\ p1Q1(3p1^2+2Q1^2+3Q3^2)y}{2C1^2K1\pi(C1+Q1^2)^{3/2}}+\frac{b_yc\ p1Q2(3p1^2+2Q2^2+3Q3^2)y}{2A4^{3/2}C1^2K1\pi}-$$
$$\frac{b_yc\ p1Q1(3p1^2+2Q1^2+3Q4^2)y}{2C2^2K1\pi(C2+Q1^2)^{3/2}}-\frac{b_yc\ p1Q2(3p1^2+2Q2^2+3Q4^2)y}{2A3^{3/2}C2^2K1\pi}+\frac{3b\ b_yc\ p1^2Q1z}{4C1K1\pi(C1+Q1^2)^{5/2}}+\frac{3b\ b_yc\ p1^2Q1z}{4C2K1\pi(C2+Q1^2)^{5/2}}+\frac{3b\ b_yc\ p1^2Q2z}{4A4^{5/2}C1K1\pi}+$$
$$\frac{3b\ b_yc\ p1^2Q2z}{4A3^{5/2}C2K1\pi}+\frac{3b_yc\ p1^2Q1yz}{4C1K1\pi(C1+Q1^2)^{5/2}}-\frac{3b_yc\ p1^2Q1yz}{4C2K1\pi(C2+Q1^2)^{5/2}}+\frac{3b_yc\ p1^2Q2yz}{4A4^{5/2}C1K1\pi}-\frac{3b_yc\ p1^2Q2yz}{4A3^{5/2}C2K1\pi}-$$
$$\frac{b\ b_yc\ Q1(3p1^2+2Q1^2+3Q3^2)(p6(c^2+Q3^2)-z^3)}{4C1^3K1\pi(C1+Q1^2)^{3/2}}-\frac{b\ b_yc\ Q2(3p1^2+2Q2^2+3Q3^2)(p6(c^2+Q3^2)-z^3)}{4A4^{3/2}C1^3K1\pi}-$$
$$\frac{b_yc\ Q1(3p1^2+2Q1^2+3Q3^2)y(p6(c^2+Q3^2)-z^3)}{4C1^3K1\pi(C1+Q1^2)^{3/2}}-\frac{b_yc\ Q2(3p1^2+2Q2^2+3Q3^2)y(p6(c^2+Q3^2)-z^3)}{4A4^{3/2}C1^3K1\pi}-$$
$$\frac{b\ b_yc\ Q1(3p1^2+2Q1^2+3Q4^2)(p6(c^2+Q4^2)-z^3)}{4C2^3K1\pi(C2+Q1^2)^{3/2}}-\frac{b\ b_yc\ Q2(3p1^2+2Q2^2+3Q4^2)(p6(c^2+Q4^2)-z^3)}{4A3^{3/2}C2^3K1\pi}+$$
$$\frac{b_yc\ Q1(3p1^2+2Q1^2+3Q4^2)y(p6(c^2+Q4^2)-z^3)}{4C2^3K1\pi(C2+Q1^2)^{3/2}}+\frac{b_yc\ Q2(3p1^2+2Q2^2+3Q4^2)y(p6(c^2+Q4^2)-z^3)}{4A3^{3/2}C2^3K1\pi};$$

Considering the Burgers vector component b_z:

$$\epsilon_{xx}=$$
$$-\frac{3a\ b_zc\ \ p1^2Q3z}{4A2^{5/2}B1K1\pi}-\frac{3a\ b_zc\ p1^2Q3z}{4A4^{5/2}B2K1\pi}+\frac{3a\ b_zc\ p1^2Q4z}{4A1^{5/2}B1K1\pi}+\frac{3a\ b_zc\ p1^2Q4z}{4A3^{5/2}B2K1\pi}+\frac{3\ b_zc\ p1^2Q3xz}{4A2^{5/2}B1K1\pi}-\frac{3\ b_zc\ p1^2Q3xz}{4A4^{5/2}B2K1\pi}-\frac{3\ b_zc\ p1^2Q4xz}{4A1^{5/2}B1K1\pi}+$$
$$\frac{3\ b_zc\ p1^2Q4xz}{4A3^{5/2}B2K1\pi}+\frac{a\ b_zc\ Q3(p8+2cQ1^2+3Q1^2z)}{2\sqrt{A2}B1^3K1\pi}+\frac{a\ b_zc\ Q3(p8+2cQ1^2+3Q1^2z)}{4A2^{3/2}B1^2K1\pi}-\frac{a\ b_zc\ Q4(p8+2cQ1^2+3Q1^2z)}{2\sqrt{A1}B1^3K1\pi}-$$
$$\frac{a\ b_zc\ Q4(p8+2cQ1^2+3Q1^2z)}{4A1^{3/2}B1^2K1\pi}-\frac{b_zc\ Q3x(p8+2cQ1^2+3Q1^2z)}{2\sqrt{A2}B1^3K1\pi}-\frac{b_zc\ Q3x(p8+2cQ1^2+3Q1^2z)}{4A2^{3/2}B1^2K1\pi}+\frac{b_zc\ Q4x(p8+2cQ1^2+3Q1^2z)}{2\sqrt{A1}B1^3K1\pi}+$$
$$\frac{b_zc\ Q4x(p8+2cQ1^2+3Q1^2z)}{4A1^{3/2}B1^2K1\pi}+\frac{a\ b_zc\ Q3(p8+2cQ2^2+3Q2^2z)}{2\sqrt{A4}B2^3K1\pi}+\frac{a\ b_zc\ Q3(p8+2cQ2^2+3Q2^2z)}{4A4^{3/2}B2^2K1\pi}-\frac{a\ b_zc\ Q4(p8+2cQ2^2+3Q2^2z)}{2\sqrt{A3}B2^3K1\pi}-$$
$$\frac{a\ b_zc\ Q4(p8+2cQ2^2+3Q2^2z)}{4A3^{3/2}B2^2K1\pi}+\frac{b_zc\ Q3x(p8+2cQ2^2+3Q2^2z)}{2\sqrt{A4}B2^3K1\pi}+\frac{b_zc\ Q3x(p8+2cQ2^2+3Q2^2z)}{4A4^{3/2}B2^2K1\pi}-\frac{b_zc\ Q4x(p8+2cQ2^2+3Q2^2z)}{2\sqrt{A3}B2^3K1\pi}-$$
$$\frac{b_zc\ Q4x(p8+2cQ2^2+3Q2^2z)}{4A3^{3/2}B2^2K1\pi}-\frac{a\ b_zc\ p1Q3(3A2-Q3^2)\nu}{2A2^{3/2}B1^2K1\pi}-\frac{a\ b_zc\ p1Q3(3A4-Q3^2)\nu}{2A4^{3/2}B2^2K1\pi}+\frac{a\ b_zc\ p1Q4(3A1-Q4^2)\nu}{2A1^{3/2}B1^2K1\pi}+$$
$$\frac{a\ b_zc\ p1Q4(3A3-Q4^2)\nu}{2A3^{3/2}B2^2K1\pi}+\frac{b_zc\ p1Q3(3A2-Q3^2)x\nu}{2A2^{3/2}B1^2K1\pi}-\frac{b_zc\ p1Q3(3A4-Q3^2)x\nu}{2A4^{3/2}B2^2K1\pi}-\frac{b_zc\ p1Q4(3A1-Q4^2)x\nu}{2A1^{3/2}B1^2K1\pi}+\frac{b_zc\ p1Q4(3A3-Q4^2)x\nu}{2A3^{3/2}B2^2K1\pi};$$

$$\epsilon_{yy} = -\frac{3b\,b_z c\,p1^2Q1z}{4C1K1\pi(C1+Q1^2)^{5/2}} - \frac{3b\,b_z c\,p1^2Q1z}{4C2K1\pi(C2+Q1^2)^{5/2}} - \frac{3b\,b_z c\,p1^2Q2z}{4A4^{5/2}C1K1\pi} - \frac{3b\,b_z c\,p1^2Q2z}{4A3^{5/2}C2K1\pi} - \frac{3\,b_z c\,p1^2Q1yz}{4C1K1\pi(C1+Q1^2)^{5/2}} + \frac{3\,b_z c\,p1^2Q1yz}{4C2K1\pi(C2+Q1^2)^{5/2}} - \frac{3\,b_z c\,p1^2Q2yz}{4A4^{5/2}C1K1\pi} + \frac{3\,b_z c\,p1^2Q2yz}{4A3^{5/2}C2K1\pi} + \frac{b\,b_z c\,Q1(p8+2cQ3^2+3Q3^2z)}{4C1^2K1\pi(C1+Q1^2)^{3/2}} + \frac{b\,b_z c\,Q1(p8+2cQ3^2+3Q3^2z)}{2C1^3K1\pi\sqrt{C1+Q1^2}} + \frac{b\,b_z c\,Q2(p8+2cQ3^2+3Q3^2z)}{2\sqrt{A4}C1^3K1\pi} + \frac{b\,b_z c\,Q2(p8+2cQ3^2+3Q3^2z)}{4A4^{3/2}C1^2K1\pi} + \frac{b_z c\,Q1y(p8+2cQ3^2+3Q3^2z)}{4C1^2K1\pi(C1+Q1^2)^{3/2}} + \frac{b_z c\,Q1y(p8+2cQ3^2+3Q3^2z)}{2C1^3K1\pi\sqrt{C1+Q1^2}} + \frac{b_z c\,Q2y(p8+2cQ3^2+3Q3^2z)}{2\sqrt{A4}C1^3K1\pi} + \frac{b_z c\,Q2y(p8+2cQ3^2+3Q3^2z)}{4A4^{3/2}C1^2K1\pi} + \frac{b\,b_z c\,Q1(p8+2cQ4^2+3Q4^2z)}{4C2^2K1\pi(C2+Q1^2)^{3/2}} + \frac{b\,b_z c\,Q1(p8+2cQ4^2+3Q4^2z)}{2C2^3K1\pi\sqrt{C2+Q1^2}} + \frac{b\,b_z c\,Q2(p8+2cQ4^2+3Q4^2z)}{2\sqrt{A3}C2^3K1\pi} + \frac{b\,b_z c\,Q2(p8+2cQ4^2+3Q4^2z)}{4A3^{3/2}C2^2K1\pi} - \frac{b_z c\,Q1y(p8+2cQ4^2+3Q4^2z)}{4C2^2K1\pi(C2+Q1^2)^{3/2}} - \frac{b_z c\,Q1y(p8+2cQ4^2+3Q4^2z)}{2C2^3K1\pi\sqrt{C2+Q1^2}} - \frac{b_z c\,Q2y(p8+2cQ4^2+3Q4^2z)}{2\sqrt{A3}C2^3K1\pi} - \frac{b_z c\,Q2y(p8+2cQ4^2+3Q4^2z)}{4A3^{3/2}C2^2K1\pi} - \frac{b\,b_z c\,p1Q1(3p1^2+2Q1^2+3Q3^2)\nu}{2C1^2K1\pi(C1+Q1^2)^{3/2}} - \frac{b\,b_z c\,p1Q2(3p1^2+2Q2^2+3Q3^2)\nu}{2A4^{3/2}C1^2K1\pi} - \frac{b\,b_z c\,p1Q1(3p1^2+2Q1^2+3Q4^2)\nu}{2C2^2K1\pi(C2+Q1^2)^{3/2}} - \frac{b\,b_z c\,p1Q2(3p1^2+2Q2^2+3Q4^2)\nu}{2A3^{3/2}C2^2K1\pi} - \frac{b_z c\,p1Q1(3p1^2+2Q1^2+3Q3^2)y\nu}{2C1^2K1\pi(C1+Q1^2)^{3/2}} - \frac{b_z c\,p1Q2(3p1^2+2Q2^2+3Q3^2)y\nu}{2A4^{3/2}C1^2K1\pi} + \frac{b_z c\,p1Q1(3p1^2+2Q1^2+3Q4^2)y\nu}{2C2^2K1\pi(C2+Q1^2)^{3/2}} + \frac{b_z c\,p1Q2(3p1^2+2Q2^2+3Q4^2)y\nu}{2A3^{3/2}C2^2K1\pi};$$

$$\epsilon_{zz} = \frac{1}{4\pi Q1^5(1-\nu)} b_z c\,\sqrt{C1+Q1^2}Q3\left(-\frac{8p1^2Q1^4z}{C1^3} + \frac{3p1^4Q1^4z}{(C1+Q1^2)^3(p1^2+Q1^2)} + \frac{2p1^6p9Q1^2+20p1^3Q1^6+3p0Q1^8+3p1^8z+12p1^4Q1^4(c+2z)}{(C1+Q1^2)(p1^2+Q1^2)^3} - \frac{p1^2Q1^2(p1^4z+2Q1^4(2c+5z)+p1^2Q1^2(4c+7z))}{(C1+Q1^2)^2(p1^2+Q1^2)^2} + \frac{2Q1^2(2c^2z+5Q1^2z+2z^3+4c(Q1^2+z^2))}{C1^2} - \frac{3c^2z+5Q1^2z+3z^3+2c(2Q1^2+3z^2)}{C1}\right) - \frac{1}{4\pi Q1^5(1-\nu)} b_z c\,Q4\sqrt{p1^2+Q1^2+Q4^2}\left(-\frac{8p1^2Q1^4z}{(p1^2+Q4^2)^3} + \frac{3p1^4Q1^4z}{(p1^2+Q1^2)(p1^2+Q1^2+Q4^2)^3} + \frac{2p1^6p9Q1^2+20p1^3Q1^6+3p0Q1^8+3p1^8z+12p1^4Q1^4(c+2z)}{(p1^2+Q1^2)^3(p1^2+Q1^2+Q4^2)} - \frac{p1^2Q1^2(p1^4z+2Q1^4(2c+5z)+p1^2Q1^2(4c+7z))}{(p1^2+Q1^2)^2(p1^2+Q1^2+Q4^2)^2} + \frac{2Q1^2(2c^2z+5Q1^2z+2z^3+4c(Q1^2+z^2))}{(p1^2+Q4^2)^2} - \frac{3c^2z+5Q1^2z+3z^3+2c(2Q1^2+3z^2)}{p1^2+Q4^2}\right) + \frac{1}{4\pi Q2^5(1-\nu)}\sqrt{A4}b_z c\,Q3\left(-\frac{8p1^2Q2^4z}{C1^3} + \frac{3p1^4Q2^4z}{A4^3B2} + \frac{2p1^6p9Q2^2+20p1^3Q2^6+3p0Q2^8+3p1^8z+12p1^4Q2^4(c+2z)}{A4B2^3} - \frac{p1^2Q2^2(p1^4z+2Q2^4(2c+5z)+p1^2Q2^2(4c+7z))}{A4^2B2^2} + \frac{2Q2^2(2c^2z+5Q2^2z+2z^3+4c(Q2^2+z^2))}{C1^2} - \frac{3c^2z+5Q2^2z+3z^3+2c(2Q2^2+3z^2)}{C1}\right) - \frac{1}{4\pi Q2^5(1-\nu)}\sqrt{A3}b_z cQ4\left(\frac{3p1^4Q2^4z}{A3^3B2} - \frac{8p1^2Q2^4z}{(p1^2+Q4^2)^3} + \frac{2p1^6p9Q2^2+20p1^3Q2^6+3p0Q2^8+3p1^8z+12p1^4Q2^4(c+2z)}{A3B2^3} - \frac{p1^2Q2^2(p1^4z+2Q2^4(2c+5z)+p1^2Q2^2(4c+7z))}{A3^2B2^2} + \frac{2Q2^2(2c^2z+5Q2^2z+2z^3+4c(Q2^2+z^2))}{(p1^2+Q4^2)^2} - \frac{3c^2z+5Q2^2z+3z^3+2c(2Q2^2+3z^2)}{p1^2+Q4^2}\right) + \frac{1}{2\pi(1-\nu)} b_z c\left(\frac{p1\sqrt{C1+Q1^2}Q3}{Q1^3}\left(\frac{1}{C1} - \frac{2Q1^2}{C1^2} + \frac{p1^2Q1^2}{(C1+Q1^2)^2(p1^2+Q1^2)} - \frac{p1^4+2p1^2Q1^2+3Q1^4}{(C1+Q1^2)(p1^2+Q1^2)^2}\right) + \frac{\sqrt{A4}p1Q3}{Q2^3}\left(\frac{1}{C1} - \frac{2Q2^2}{C1^2} + \frac{p1^2Q2^2}{A4^2B2} - \frac{p1^4+2p1^2Q2^2+3Q2^4}{A4B2^2}\right) - \frac{\sqrt{A3}p1Q4}{Q2^3}\left(\frac{p1^2Q2^2}{A3^2B2} - \frac{p1^4+2p1^2Q2^2+3Q2^4}{A3B2^2} - \frac{2Q2^2}{(p1^2+Q4^2)^2} + \frac{1}{p1^2+Q4^2}\right) - \frac{p1Q4\sqrt{p1^2+Q1^2+Q4^2}}{Q1^3}\left(-\frac{2Q1^2}{(p1^2+Q4^2)^2} + \frac{1}{p1^2+Q4^2} + \frac{p1^2Q1^2}{(p1^2+Q1^2)(p1^2+Q1^2+Q4^2)^2} - \frac{p1^4+2p1^2Q1^2+3Q1^4}{(p1^2+Q1^2)^2(p1^2+Q1^2+Q4^2)}\right)\right)(2(1-\nu)+\nu);$$

$$\epsilon_{xy} = \frac{b_z c}{4K1\pi}\left(\frac{-2c-3z}{A1^{3/2}} + \frac{3p1^2z}{A1^{5/2}} - \frac{3p1^2z}{A3^{5/2}} + \frac{2c+3z}{A3^{3/2}}\right) - \frac{b_z c}{4K1\pi}\left(\frac{-2c-3z}{A2^{3/2}} + \frac{3p1^2z}{A2^{5/2}} - \frac{3p1^2z}{A4^{5/2}} + \frac{2c+3z}{A4^{3/2}}\right) + \frac{b_z c\,p1\nu}{2K1\pi}\left(\frac{1}{A1^{3/2}} - \frac{1}{A3^{3/2}}\right) - \frac{b_z c\,p1\nu}{2K1\pi}\left(\frac{1}{A2^{3/2}} - \frac{1}{A4^{3/2}}\right);$$

$$\epsilon_{xz} = \frac{b_z c\,p1^2Q3}{2A2^{3/2}B1K1\pi} - \frac{b_z c\,p1^2Q3}{2A4^{3/2}B2K1\pi} - \frac{b_z c\,p1^2Q4}{2A1^{3/2}B1K1\pi} + \frac{b_z c\,p1^2Q4}{2A3^{3/2}B2K1\pi} - \frac{b_z c\,Q3(Q1^2-p1^2)}{2\sqrt{A2}B1^2K1\pi} + \frac{b_z c\,Q4(Q1^2-p1^2)}{2\sqrt{A1}B1^2K1\pi} + \frac{b_z c\,Q3(Q2^2-p1^2)}{2\sqrt{A4}B2^2K1\pi} - \frac{b_z c\,Q4(Q2^2-p1^2)}{2\sqrt{A3}B2^2K1\pi} + \frac{3b_z c\,p1^3Q3z}{4A2^{5/2}B1K1\pi} - \frac{3b_z c\,p1^3Q3z}{4A4^{5/2}B2K1\pi} - \frac{3b_z c\,p1^3Q4z}{4A1^{5/2}B1K1\pi} + \frac{3b_z c\,p1^3Q4z}{4A3^{5/2}B2K1\pi} - \frac{b_z c\,p1Q3(p1^2p3+3a^2(c+2z)-6ax(c+2z)+3x^2(c+2z))}{4A2^{3/2}B1^2K1\pi} + \frac{b_z c\,p1Q4(p1^2p3+3a^2(c+2z)-6ax(c+2z)+3x^2(c+2z))}{4A1^{3/2}B1^2K1\pi} - \frac{b_z c\,Q3(-3a^4+p1^3p5+12a^3x-3x^4+6p1x^2z+12ax(x^2-p1z)+6a^2(-3x^2+p1z))}{4\sqrt{A2}B1^3K1\pi} + \frac{b_z c\,Q4(-3a^4+p1^3p5+12a^3x-3x^4+6p1x^2z+12ax(x^2-p1z)+6a^2(-3x^2+p1z))}{4\sqrt{A1}B1^3K1\pi} + \frac{b_z c\,Q3(-3a^4+p1^3p5-12a^3x-3x^4+6p1x^2z+6a^2(-3x^2+p1z)+12ax(-x^2+p1z))}{4\sqrt{A4}B2^3K1\pi} -$$

$$\frac{b_z c\ Q4(-3a^4+p1^3p5-12a^3x-3x^4+6p1x^2z+6a^2(-3x^2+p1z)+12ax(-x^2+p1z))}{4\sqrt{A3}B2^3K1\pi}+\frac{b_z c\ p1Q3(3c^3+8c^2z+6Q2^2z+2z^3+c(3Q2^2+7z^2))}{4A4^{3/2}B2^2K1\pi}-$$
$$\frac{b_z c\ p1Q4(3c^3+8c^2z+6Q2^2z+2z^3+c(3Q2^2+7z^2))}{4A3^{3/2}B2^2K1\pi};$$

$$\epsilon_{yz}=$$
$$-\frac{b_z c\ p1^2Q1}{2C1K1\pi(C1+Q1^2)^{3/2}}+\frac{b_z c\ p1^2Q1}{2C2K1\pi(C2+Q1^2)^{3/2}}-\frac{b_z c\ p1^2Q2}{2A4^{3/2}C1K1\pi}+\frac{b_z c\ p1^2Q2}{2A3^{3/2}C2K1\pi}+\frac{b_z c\ Q1(Q3^2-p1^2)}{2C1^2K1\pi\sqrt{C1+Q1^2}}+\frac{b_z c\ Q2(Q3^2-p1^2)}{2\sqrt{A4}C1^2K1\pi}-$$
$$\frac{b_z c\ Q1(Q4^2-p1^2)}{2C2^2K1\pi\sqrt{C2+Q1^2}}-\frac{b_z c\ Q2(Q4^2-p1^2)}{2\sqrt{A3}C2^2K1\pi}-\frac{3b_z c\ p1^3Q1z}{4C1K1\pi(C1+Q1^2)^{5/2}}+\frac{3b_z c\ p1^3Q1z}{4C2K1\pi(C2+Q1^2)^{5/2}}-\frac{3b_z c\ p1^3Q2z}{4A4^{5/2}C1K1\pi}+\frac{3b_z c\ p1^3Q2z}{4A3^{5/2}C2K1\pi}-$$
$$\frac{b_z c\ p1Q1(p1^2p3+3b^2(c+2z)-6by(c+2z)+3y^2(c+2z))}{4C2^2K1\pi(C2+Q1^2)^{3/2}}-\frac{b_z c\ p1Q2(p1^2p3+3b^2(c+2z)-6by(c+2z)+3y^2(c+2z))}{4A3^{3/2}C2^2K1\pi}-$$
$$\frac{b_z c\ Q1(-3b^4+p1^3p5+12b^3y-3y^4+6p1y^2z+12by(y^2-p1z)+6b^2(-3y^2+p1z))}{4C2^3K1\pi\sqrt{C2+Q1^2}}-$$
$$\frac{b_z c\ Q2(-3b^4+p1^3p5+12b^3y-3y^4+6p1y^2z+12by(y^2-p1z)+6b^2(-3y^2+p1z))}{4\sqrt{A3}C2^3K1\pi}+$$
$$\frac{b_z c\ Q1(-3b^4+p1^3p5-12b^3y-3y^4+6p1y^2z+6b^2(-3y^2+p1z)+12by(-y^2+p1z))}{4C1^3K1\pi\sqrt{C1+Q1^2}}+$$
$$\frac{b_z c\ Q2(-3b^4+p1^3p5-12b^3y-3y^4+6p1y^2z+6b^2(-3y^2+p1z)+12by(-y^2+p1z))}{4\sqrt{A4}C1^3K1\pi}+\frac{b_z c\ p1Q1(3c^3+8c^2z+6Q3^2z+2z^3+c(3Q3^2+7z^2))}{4C1^2K1\pi(C1+Q1^2)^{3/2}}+$$
$$\frac{b_z c\ p1Q2(3c^3+8c^2z+6Q3^2z+2z^3+c(3Q3^2+7z^2))}{4A4^{3/2}C1^2K1\pi};$$

$$p1=zp+z=c+z;$$
$$p2=z-zp=z-c;$$
$$p3=2z+3zp=2z+3c;$$
$$p4=6z+3zp=6z+3c;$$
$$p5=z+3zp=z+3c;$$
$$p6=3z+2zp=3z+2c;$$
$$p7=-3z-2zp=-3z-2c;$$
$$p8=-z^3+3zzp^2+2zp^3=-z^3+3zc^2+2c^3;$$
$$p9=7z+2zp=7z+2c;$$
$$p0=5z+4zp=5z+4c;$$
$$A1=p1^2+(a-x)^2+(b-y)^2;$$
$$A2=p1^2+(a-x)^2+(b+y)^2;$$
$$A3=p1^2+(a+x)^2+(b-y)^2;$$
$$A4=p1^2+(a+x)^2+(b+y)^2;$$
$$B1=p1^2+(a-x)^2;$$
$$B2=p1^2+(a+x)^2;$$
$$C1=p1^2+(b+y)^2;$$
$$C2=p1^2+(b-y)^2;$$
$$K1=-1+\nu;$$
$$K2=-1+2\nu;$$
$$K3=-2+\nu;$$
$$Q1=a-x;$$
$$Q2=a+x;$$
$$Q3=b+y;$$
$$Q4=-b+y;$$

© 2021 Li and Khraishi; This is an Open Access article distributed under the terms of the Creative Commons Attribution License (http://creativecommons.org/licenses/by/4.0), which permits unrestricted use, distribution, and reproduction in any medium, provided the original work is properly cited.

Peer-review history:
The peer review history for this paper can be accessed here:
http://www.sdiarticle4.com/review-history/65917